ON THE FEASIBILITY OF USING SUPERCRITICAL CO_2 AS HEAT TRANSMISSION FLUID IN AN ENGINEERED HOT DRY ROCK GEOTHERMAL SYSTEM

Karsten Pruess[1] and Mohamed Azaroual[2]

1 Earth Sciences Division, Lawrence Berkeley National Laboratory, Berkeley, CA 94720, U.S.A.
2 BRGM - Water Division, 3 av. C. Guillemin, BP 6009, F-45060 Orléans Cedex 2, FRANCE
K_Pruess@lbl.gov, M.Azaroual@brgm.fr

ABSTRACT

Responding to the need to reduce atmospheric emissions of carbon dioxide, Donald Brown (2000) proposed a novel hot dry rock (HDR) concept that would use CO_2 as heat transmission fluid, and would achieve geologic sequestration of CO_2 as an ancillary benefit. Following up on his suggestion, we have evaluated thermophysical properties and performed numerical simulations to explore the fluid dynamics and heat transfer issues in a HDR reservoir that would be operated with CO_2. We find that CO_2 is roughly comparable to water in its ability to mine heat from hot fractured rock. CO_2 has certain advantages with respect to wellbore hydraulics, where larger compressibility and expansivity and lower viscosity as compared to water would reduce the parasitic power consumption of the fluid circulation system. Chemical interactions induced by CO_2 between fluids and rocks suggest a potential for porosity enhancement and reservoir growth. A HDR system running on CO_2 has sufficiently attractive features to warrant further investigation.

INTRODUCTION

Responding to the need to reduce atmospheric emissions of carbon dioxide, Donald Brown (2000) proposed a novel hot dry rock (HDR) concept that would use CO_2 instead of water as heat transmission fluid, and would achieve geologic storage of CO_2 as an ancillary benefit. Brown noted that CO_2 has certain physical and chemical properties that would be favorable for operation of a HDR system. Favorable properties of CO_2 emphasized by Brown include the following:

- large expansivity would generate large density differences between the cold CO_2 in the injection well and the hot CO_2 in the production well, and would provide buoyancy force that would reduce the power consumption of the fluid circulation system;
- lower viscosity would yield larger flow velocities for a given pressure gradient; and
- CO_2 would be much less effective as a solvent for rock minerals, which would reduce or eliminate scaling problems, such as silica dissolution and precipitation in water-based systems.

Brown also noted the lower mass heat capacity of CO_2 as an unfavorable property, but pointed out that this would be partially compensated by the greater flow capacity of CO_2 due to lower viscosity. Fouillac et al. (2004) suggested that an enhanced geothermal system (EGS) using CO_2 as heat transmission fluid could have favorable geochemical properties, as CO_2 uptake and sequestration by rock minerals would be quite rapid at elevated temperatures.

The present paper compares thermophysical properties of CO_2 and water, and examines pressure and temperature conditions for flow of CO_2 in wellbores as well as in reservoirs with predominant fracture permeability. Comparisons are made with the flow behavior of water, in order to identify favorable as well as unfavorable characteristics of CO_2 as a HDR working fluid. We also present preliminary considerations on chemical aspects of a CO_2-HDR system.

THERMOPHYSICAL PROPERTIES

Fig. 1 shows the phase diagram for CO_2 in the range of temperature and pressure conditions that are of interest for injection into and production from enhanced geothermal systems. The critical point of CO_2 is at $T_{crit} = 31.04$ °C, $P_{crit} = 73.82$ bar (Vargaftik, 1975). At lower (subcritical) temperatures and/or pressures, CO_2 can exist in two different

phases, a liquid and a gaseous state, as well as two-phase mixtures of these states (Fig. 1). Supercritical CO_2 forms a phase that is distinct from the aqueous phase and can change continuously into either gaseous or liquid CO_2 with no phase boundaries.
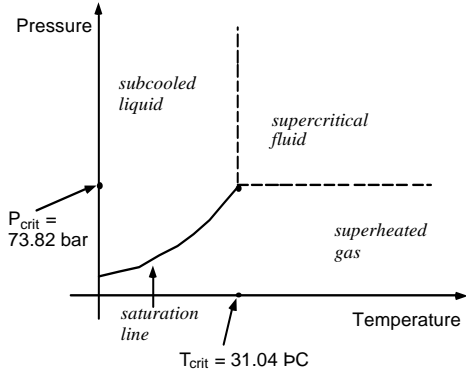

Figure 1. Phase states of CO_2.

Fluid mass flow rates for a given driving force are proportional to the ratio of density to viscosity, m = ρ/μ (Fig. 2). The sensible heat carried by mass flow is proportional to the specific enthalpy of the fluid (Fig. 3). Additional parameters that are important for mass flow and heat transfer behavior include compressibility $c = (1/\rho)(\partial\rho/\partial P)$ and thermal expansivity $\varepsilon = -(1/\rho)(\partial\rho/\partial T)$.

CO_2 properties in Figs. 2 and 3 were calculated from the correlations of Altunin (Altunin, 1975; Pruess and García, 2002). We began using Altunin's correlations in 1999 when a computer program implementing them was kindly made available to us by Victor Malkovsky of the Institute of Geology of Ore Deposits, Petrography, Mineralogy and Geochemistry (IGEM) of the Russian Academy of Sciences, Moscow. Altunin's correlations were subsequently extensively cross-checked against experimental data and alternative PVT formulations, such as Span and Wagner (1996), and were found to be very accurate (García, 2003). Water properties were obtained from the steam table equations as given by the International Formulation Committee (IFC, 1967).

The ratio of density to viscosity is generally larger for CO_2 than for water, and dependence on temperature and pressure conditions is very different for the two fluids (Fig. 2). For water this ratio is mostly a function of temperature, with only weak dependence on pressure, reflecting the primary dependence of both water density and viscosity on temperature. For CO_2, density and viscosity have significant dependence on both temperature and pressure. The

variations are such that (ρ/μ) attains maximum values in a region that is emanating from the CO_2 saturation line, becoming smaller for liquid-like CO_2 (low T, high P) and for gas-like CO_2 (high T, low P). For (T, P)- conditions relevant for fluid injection, T $\leq$ 50 °C, (ρ/μ) for CO_2 is larger than for water by factors of 4-10. For temperatures near 200 °C, (ρ/μ) for CO_2 is larger than for water by approximately a factor 2 at high pressures, while at pressures below 150 bar, water has the larger (ρ/μ).
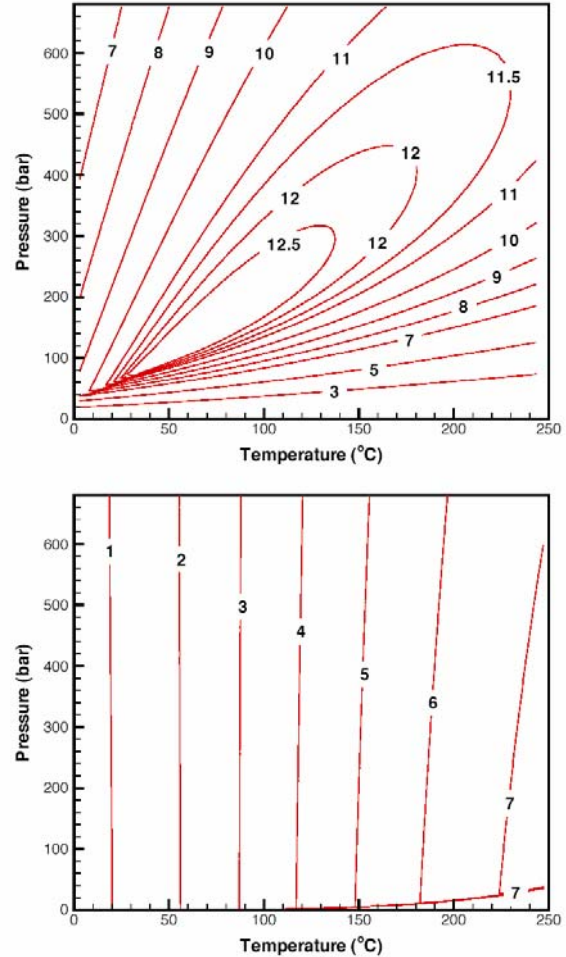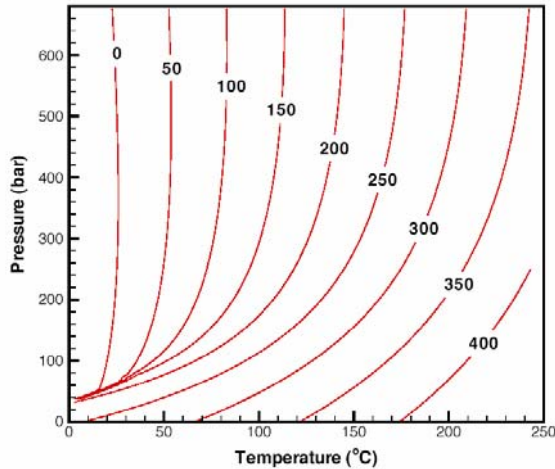

Figure 2. Ratio of fluid density to viscosity in units of 10^6 sm^{-2} for CO_2 (top) and water (bottom).

Fig. 3 compares the specific enthalpies for CO_2 and water. In both cases the reference state (zero enthalpy) was chosen as (T, P) = (20 °C, 100 bar). At high pressures near 500 bar, the increase of specific enthalpy with temperature for CO_2 is less than half of the increase for water, indicating that more than twice the CO_2 mass flow rate would be needed to achieve the same rate of sensible heat transport. Specific enthalpy of liquid water depends primarily on temperature, with only a weak pressure dependence.

For CO_2 the pressure dependence is weak for liquid-like conditions, but becomes increasingly strong at lower pressures and higher temperatures. For adiabatic (thermally insulated) decompression, thermodynamic conditions will move along isenthalps (lines of constant specific enthalpy). Accordingly, decompression of hot, high-pressure CO_2 will be accompanied by substantial temperature decline, while for liquid water there would be a small temperature increase.
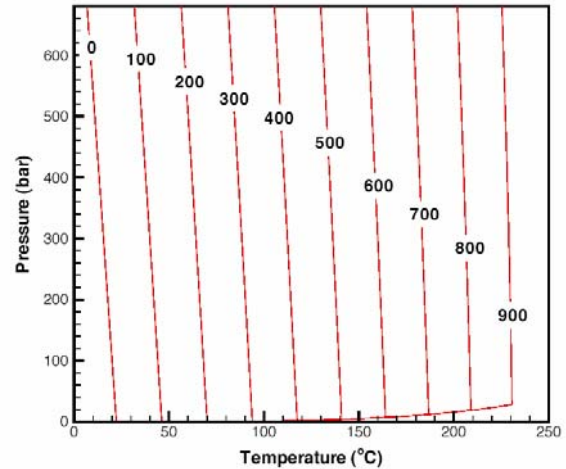

Figure 3. Specific enthalpy of CO_2 (left) and water (right) in units of kJ/kg, as function of temperature and pressure.

WELLBORE FLOW

The pressure gradient in a flowing well can be represented by a superposition of gravity, frictional, and acceleration terms (Brill and Mukherjee, 1999),

$$\nabla P = (\nabla P)_{grav} + (\nabla P)_{fric} + (\nabla P)_{acc} \qquad (1)$$

For most applications of interest, the gravitational contribution to the pressure gradient is by far the dominant term, with frictional and inertial pressure gradients contributing typically a few percent or less. In a first effort to evaluate the pressures in HDR injection and production wells, we consider only the dominant gravitational gradient.

In an injection well, temperatures will increase with depth, primarily because of heat transfer from the surrounding rocks (Ramey, 1962). Additional temperature changes are expected as a consequence of fluid compression due to pressure increase. The latter effect is very small for water, but could be more significant for the highly compressible CO_2. Similarly, in a production well the temperature of a fluid parcel flowing upward will decrease due to heat loss to the surrounding formations. Additional temperature change will occur from decompression, which is expected to be a small effect for water, but could be significant for CO_2.

The temperature effects from heat exchange with the surroundings are of a transient nature and will diminish over time. For a basic comparison between the pressure behavior of water and CO_2 wells, we start from the simplest possible approximation to temperature conditions: we consider an injection well that is entirely at the injection (wellhead) temperature T_{inj}, and a production well that is entirely at the production (downhole) temperature T_{pro}. In order to calculate the static pressure profile in a well, the well depth z is divided into N increments, $\Delta z = z/N$. The calculation proceeds recursively from level $n\Delta z$ to $(n+1)\Delta z$ by assigning $P_{n+1} = P_n + \rho_n g\Delta z$, where $\rho_n = \rho(T_n, P_n)$, and $g = 9.81$ m^2/s is gravitational acceleration. For definiteness, we adopt parameters applicable to the European HDR experiment at Soultz, and take a well depth of 5,000 m, with a downhole temperature of $T_{pro} = 200$ ˚C (Baria et al., 2005; Dezayes et al., 2005). Injection temperature is set at $T_{inj} = 20$ ˚C.

For both water and CO_2 we start from an injection wellhead pressure of 57.4 bar, slightly in excess of the CO_2 saturation pressure at injection temperature ($P_{sat,CO2} = 57.36$ bar at $T_{inj} = 20$ ˚C). Corresponding static downhole pressures at 5,000 m depth are 528.7 bar for CO_2 and 553.4 bar for water (Fig. 4). Using these downhole pressures as starting values, we then obtain static pressures in the production well by integrating upwards at $T = 200$ ˚C. This results in production wellhead pressures of 288.1 bar for CO_2 and 118.6 bar for water. The difference in wellhead pressures between production and injection wells is 230.7 bar for CO_2 and 61.2 bar for water, indicating

that a CO_2 circulation system would have far stronger buoyant drive, and would require less power to operate.
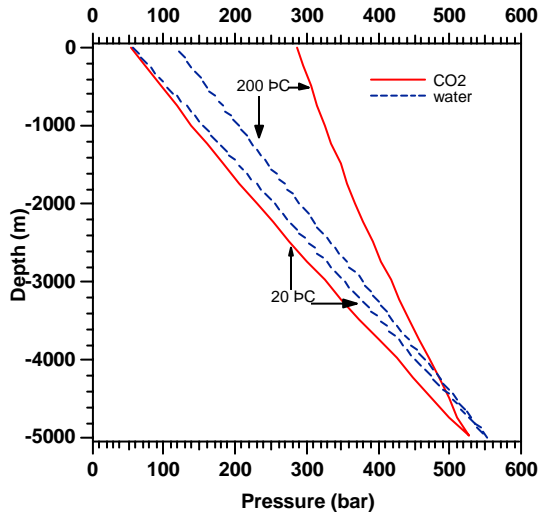

Figure 4. Static pressure profiles in CO_2 and water wells for constant temperatures of 20 and 200 ˚C, respectively.

A more realistic outlook on longer-term P,T-conditions in flowing injection and production wells can be obtained by approximating fluid flow in the wellbore as isenthalpic. This approximation is often referred to as "adiabatic;" it ignores heat transfer between the wellbore fluid and the surroundings, which is appropriate for longer-term flow behavior. The isenthalpic flow approximation accounts for temperature changes that arise from (de-)compression of fluids, the so-called Joule-Thomson effect (Katz and Lee, 1990).

We have calculated pressure and temperature conditions in a static, isenthalpic column of CO_2, using a similar recursion as for the constant-temperature wells considered above, except that now we account for temperature variation with depth as well, based on constant specific enthalpy. For an injection well, we perform a "top down" calculation starting from wellhead conditions of (T_0, P_0), corresponding to a specific enthalpy of $h_0 = h(T_0, P_0)$. At depth level n we have conditions of (T_n, P_n), from which we obtain $\rho_n = \rho(T_n, P_n)$ and $P_{n+1} = P_n + \rho_n g \Delta z$, just as before. The temperature at level n+1 is obtained as $T_{n+1} = T(P_{n+1}, h_0)$; the required inversion of the h = h(T, P) relationship is accomplished by Newtonian iteration, using T_n as a starting guess. Fig. 5 shows (T, P)-profiles in a 5000 m deep injection well for several different wellhead temperatures and pressures. Fig. 6 shows (T, P)-profiles in a 5000 m

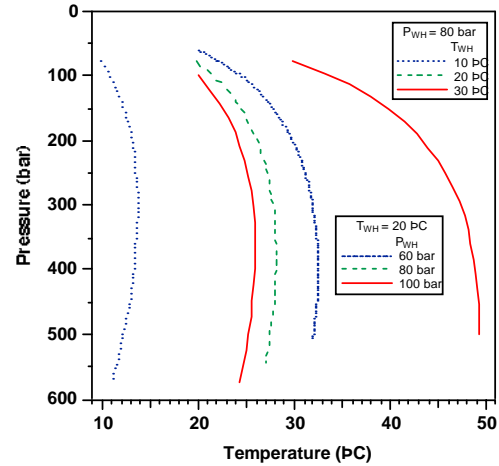deep production well for different downhole conditions.

Figure 5. Temperature-pressure conditions for isenthalpic flow of CO_2 in a 5000 m deep injection well, for different wellhead temperatures and pressures.
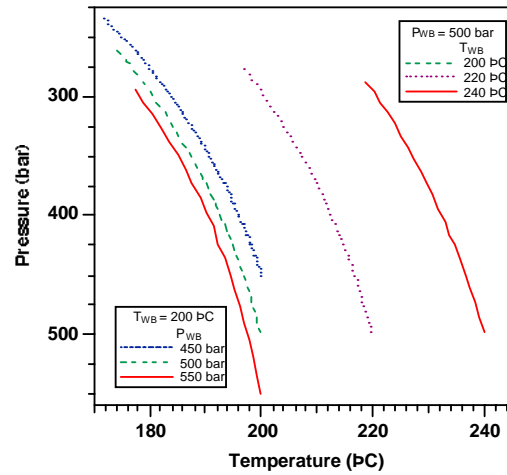

Figure 6. Temperature-pressure conditions for isenthalpic flow of CO_2 in a 5000 m deep production well, for different downhole temperatures and pressures.

Fig. 5 indicates that temperatures will tend to increase as CO_2 is flowing down the injection well and attaining increasing pressures. The difference between downhole and wellhead temperatures is larger for smaller wellhead pressures, and increases strongly when wellhead temperatures are increased. For the lower wellhead temperature cases shown in Fig. 5, temperature changes versus depth are non-monotonic, with significant temperature decline at greater depth, especially when wellhead temperature is low and/or wellhead pressure is large.

These features can be understood from the dependence of specific enthalpy of CO_2 on temperature and pressure, see Fig. 3. For adiabatic (de-)compression processes, thermodynamic conditions will move along lines of constant enthalpy, indicating that compression starting from modest pressures and/or elevated temperatures will be accompanied by strong temperature increases. At temperatures below 50 ˚C, however, the isenthalps shown in Fig. 3 curve slightly backwards towards lower temperatures at high pressures, so that in this region isenthalpic compression will be accompanied by a temperature decline.

Increased downhole temperatures in the injection well are favorable from the viewpoint of reservoir heat extraction, but they also reduce the pressure increase with depth in the injection well. This will reduce the buoyant pressure drive available for pushing CO_2 through the HDR reservoir, and will increase the power requirements for maintaining fluid circulation.

Analogous considerations apply to temperature and pressure behavior in production wells (Fig. 6). Here the isenthalpic decompression will cause CO_2 temperatures to decline as it flows up the well. The temperature drop along the well becomes stronger for smaller downhole pressures; at T_{WB} = 200 ˚C the temperature drops are ΔT = -22.6 ˚C for P_{WB} = 550 bar, -25.7 ˚C at P_{WB} = 500 bar, and -28.7 ˚C at P_{WB} = 450 bar. Temperature declines become smaller for increased downhole temperature. In the production well it is of course desirable to reduce temperature decline during fluid upflow as much as possible. This can be achieved by increasing downhole pressures, which however will require increased power consumption in the fluid circulation systems.

From this discussion it is apparent that optimal operation of a CO_2-HDR system will involve complex tradeoffs between reservoir heat extraction and power consumption in the fluid circulation system.

Fig. 7 presents static pressure profiles in CO_2 injection wells for 80 bar wellhead pressure and different wellhead temperatures. Downhole pressures decrease with increasing wellhead temperatures, and more so for adiabatic than for constant temperature conditions. This is because for adiabatic conditions wellbore temperatures are larger, and accordingly fluid densities are smaller. The differences in downhole pressures range from 5.3 to 33.3 bar (Table 1).
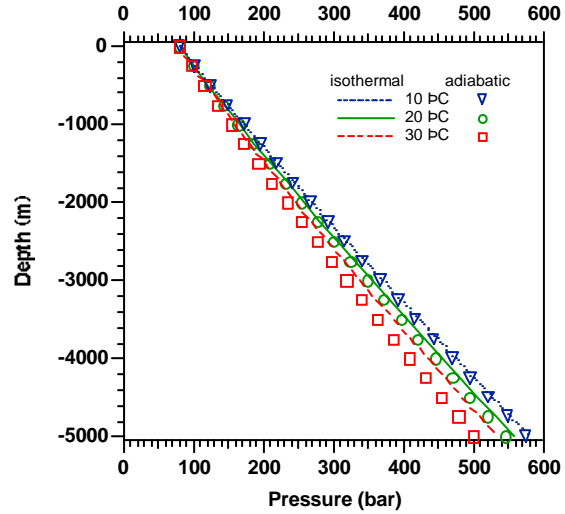

Figure 7. Static pressure profiles in CO_2 injection wells for 80 bar wellhead pressure and different wellhead temperatures. Profiles are shown for isothermal as well as adiabatic conditions.

Table 1. Downhole pressures in CO_2 injection wells for 80 bar wellhead pressure and different wellhead temperatures, for adiabatic and isothermal conditions.

T (˚C)	P_{ad} (bar)	P_{isoth} (bar)	ΔP (bar)
10	574.09	579.42	5.33
20	545.57	558.58	13.01
30	500.79	534.13	33.34

RESERVOIR HEAT EXTRACTION

Production-Injection in Single Fracture

In order to compare CO_2 and water as heat transmission fluids, we consider an idealized fractured reservoir problem whose parameters were loosely patterned after conditions at the European HDR site at Soultz (see Table 2; Baria et al., 2005; Dezayes et al., 2005). We consider a horizontal fracture zone of 700x50 m² areal extent, with injection and production occurring at a fixed pressure drop of 20 bar over 650 m distance. The wall rocks are modeled as semi-infinite half-spaces with uniform initial temperature of 200 ˚C, and the semi-analytical technique of Vinsome and Westerveld (1980) is used to calculate the heat transfer from the wall rocks to the fluid flowing in the fracture.

Table 2. Specifications of fracture injection-production problem.

Fracture zone	
thickness	0.04 m
size	50 m wide by 700 m long
permeability	200×10^{-12} m^2 (200 darcy)
porosity*	0.5
rock grain density	2650 kg/m^3
rock specific heat	1000 J/kg/$^\circ$C
rock thermal conductivity	2.1 W/m/$^\circ$C
Initial conditions	
temperature	200 $^\circ$C
pressure	500 bar
Production/injection	
injector-producer distance	650 m
injection temperature	20 $^\circ$C
injection pressure (downhole)	510 bar
production pressure (downhole)	490 bar

* we include some wall rock in the definition of the fracture domain

This problem is run in two variations, using either CO_2 or H_2O as reservoir fluid. The simulations use our TOUGH2 code with a special fluid property module "EOSM" for mixtures of water and CO_2 (Pruess, 2004a, 2004b). After a brief initial transient, production flow rates stabilize at approximately $F_{CO2} \approx 11.5$ and $F_w \approx 3$ kg/s for CO_2 and water, respectively. Net heat extraction rates were calculated as $G_i = F_i h_i - (F_i h_i)_{inj}$ (i = CO_2, water), where injection enthalpy $h_{i,inj}$ was evaluated at downhole conditions of (T, P) = (20 $^\circ$C, 510 bar). Fig. 8 shows simulated rates of net heat extraction as function of time, along with cumulative net heat extraction. It is
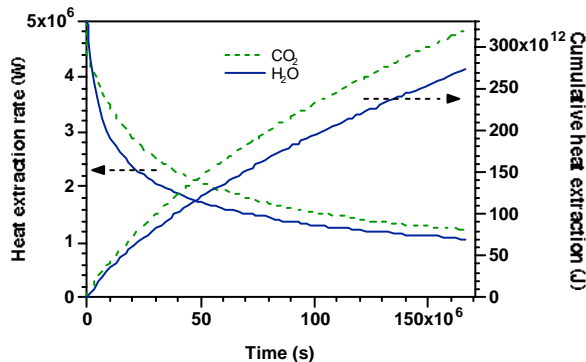

Fig. 8. Rate of heat extraction and cumulative heat produced for the fracture injection-production problem.

seen that heat extraction with CO_2 is somewhat more rapid than with water. The differences are rather small, however, indicating that the favorable and unfavorable differences in thermophysical properties - CO_2 being less dense, less viscous, and having lower specific heat - nearly cancel out for this problem.

CHEMICAL ISSUES

Aqueous solutions of CO_2 can be quite corrosive, and can dissolve rock minerals, as well as attacking steel liners and casings used in well construction (Xu et al., 2005). However, the flowing CO_2 stream would quickly dissolve *in situ* water and thereby remove the aqueous phase from the central zone of an engineered HDR reservoir. This region would be surrounded by a two-phase halo containing a mixture of supercritical CO_2 and aqueous phase, and an outer zone with a single aqueous phase with dissolved CO_2. Continuous operation of a CO_2-HDR system would be expected to produce a rather dry CO_2 stream that would not pose corrosion problems for production wells.

Rock-fluid interactions in the absence of water

The chemical interaction of supercritical CO_2 with *in situ* rock minerals raises interesting questions. Brown (2000) suggested that CO_2 would be a far less effective solvent than water, which would reduce the potential for dissolution and subsequent reprecipitation of minerals, thereby avoiding problems of scaling and formation plugging. Fouillac et al. (2004) pointed out that reactions between minerals and CO_2 should be quite rapid at the elevated temperatures in an EGS system. They suggested that CO_2 injection into granitic rock should give rise to formation of calcite. A possible example is the carbonation of wairakite, which can be written as (wairakite + CO_2 $\Leftrightarrow$ calcite + kaolinite + 2 quartz)

$$Ca(Al_2Si_4O_{12}){:}2H_2O + CO_2(g)$$
$$\Leftrightarrow CaCO_3 + Al_2Si_2O_5(OH)_4 + 2\ SiO_2 \qquad (2)$$
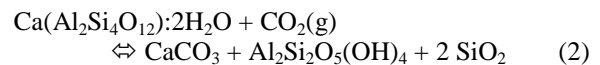
At T = 25 $^\circ$C, P = 1 atm, the molar volume of wairakite is 207.55 cm^3/mole, while the molar volumes of the reaction products sum to 181.83 cm^3/mole. This represents a volume reduction of 12.4 %, indicating that reaction (2) would cause an increase in reservoir porosity and permeability. For other minerals, prolonged exposure to supercritical CO_2 may cause dehydration reactions that would remove loosely bound water. Such reactions would tend to reduce the molar volume of the minerals involved, which would increase porosity and permeability of the formations, and may promote reservoir growth.

Rock-fluid interactions in the presence of an aqueous phase

The natural Soultz fluid is of Na-Cl-Ca-HCO$_3$ type and highly saline (~ 100 g/l) with a temperature of 200 °C and pressure near 600 bars at 5000 m (in GPK-1). The main chemical components of the brine have the following molal concentrations: [Na] = 1.27; [K] = 0.09; [Ca] = 0.17; [Cl] = 1.72; [Mg] = 6.38 10^{-3}; [SO$_4$] = 1.26 10^{-3}= [Sr] = 5.66 10^{-3}; [Ba] = 4.97 10^{-4} ; [Fe] = 7.17 10^{-4} and [CO$_2$]$_T$ = 0.019. The *in situ* conditions of pH and pCO$_2$ and the thermodynamic equilibrium state of the Soultz brine have been assessed using the geochemical software SCALE2000 (Azaroual et al., 2004). A Pitzer approach was used for ion activities, and fugacity corrections were calculated from a new EOS formulation (Duan and Sun, 2003; Kervévan et al., 2005). The *in situ* pH and pCO$_2$ are 5.0 and 5.6 bars, respectively. The circulating fluid in fractured granite with high contact surface with alteration mineral products is initially in thermodynamic equilibrium with respect to calcite, anhydrite, strontianite, siderite, mackinawite, and quartz.

Fig. 9 shows CO$_2$ solubility and pH of Soultz brine as a function of temperature at a constant CO$_2$ partial pressure of 500 bar.
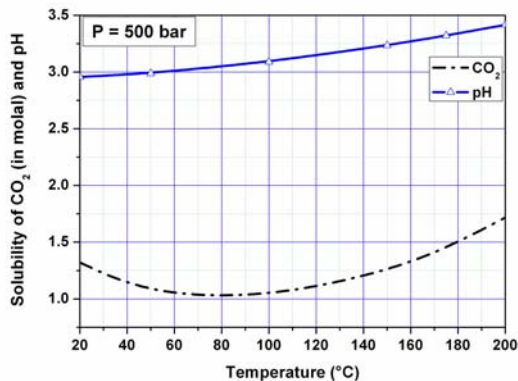

Fig. 9. *Temperature effect on the CO$_2$ solubility and pH of CO$_2$ enriched Soultz brine at 500 bar carbon dioxide partial pressure.*

The small variation of pH highlights the strong buffering capacity of Soultz brine. Fig. 10 gives a preliminary evaluation of saturation indices of major primary minerals at Soultz for CO$_2$-enriched brine. It is seen that most minerals are undersaturated at lower temperatures, suggesting that CO$_2$ injection would provide a significant potential for reservoir growth.
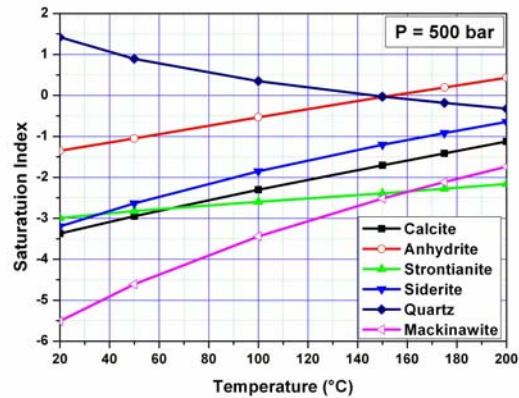

Fig. 10. *Temperature effect on the Saturation Indices (SI) of calcite, anhydrite, strontianite, siderite, quartz and mackinawite.*

CONCLUDING REMARKS

At typical temperature and pressure conditions anticipated for EGS - approximately 200 °C and a few hundred bars - CO$_2$ is a supercritical fluid with liquid-like density and gas-like viscosity. Its thermophysical properties make it quite attractive as a heat transmission fluid. Our exploratory studies suggest that CO$_2$ is roughly comparable and perhaps somewhat superior to water in its ability to mine heat from an EGS reservoir. CO$_2$ appears to offer advantages for wellbore hydraulics, which may lead to reduced power consumption for maintaining fluid circulation. Preliminary evaluation of the geochemistry of supercritical and aqueous CO$_2$ suggests a potential for mineral transformations that would be accompanied by a reduction in volume, inducing porosity increase and reservoir growth.

Fluid losses are an unavoidable aspect of engineered geothermal systems. Whereas the loss of water in a "conventional" HDR operation would be unfavorable and costly, fluid loss in a HDR system running with CO$_2$ would offer geologic storage of CO$_2$. Such storage may provide economic benefits and incentives in future carbon management scenarios. Combining EGS with CO$_2$ storage could provide an additional revenue stream that would improve the economics of EGS.

ACKNOWLEDGEMENT

REFERENCES

Altunin, V.V. (1975), *Thermophysical Properties of Carbon Dioxide,* Publishing House of Standards, 551 pp., Moscow (in Russian).

Azaroual, M., C. Kervévan, M.V. Durance, S. Brochot, and P. Durst (2004). *SCALE2000; Logiciel de calculs thermodynamiques et cinétiques applicables aux saumures pétrolières, hydrothermales et industrielles. Manuel d'Utilisation.* BRGM. ISBN 2-7159-0939-X.

Baria, R., S. Michelet, J. Baumgärtner, B. Dyer, J. Nicholls, T. Hettkamp, D. Teza, N. Soma, H. Asanuma, J. Garnish and T. Megel (2005), Creation and Mapping of 5000 m deep HDR/HFR Reservoir to Produce Electricity, *Proceedings, Paper 1627.pdf,* World Geothermal Congress 2005, Antalya, Turkey, 24-29 April.

Brill, J.P. and H. Mukherjee (1999), *Multiphase Flow in Wells,* SPE Monograph, Vol. 17, Society of Petroleum Engineers, Richardson, TX.

Brown, D. (2000), A Hot Dry Rock Geothermal Energy Concept Utilizing Supercritical CO_2 Instead of Water, *Proceedings,* Twenty-Fifth Workshop on Geothermal Reservoir Engineering, pp. 233–238, Stanford University, January.

Dezayes, C., A. Genter and G.R. Hooijkaas (2005), Deep-Seated Geology and Fracture System of the EGS Soultz Reservoir (France) based on Recent 5km Depth Boreholes, *Proceedings, Paper 1612.pdf,* World Geothermal Congress 2005, Antalya, Turkey, 24-29 April.

Duan, Z. and R. Sun (2003). An improved model calculating CO_2 solubility in pure water and aqueous NaCl solutions from 273 to 5333 K and from 0 to 2000 bar. *Chem. Geol.,* Vol. 193, 257-271.

Fouillac, C., B. Sanjuan, S. Gentier and I. Czernichowski-Lauriol (2004), Could Sequestration of CO_2 be Combined with the Development of Enhanced Geothermal Systems?, paper presented at Third Annual Conference on Carbon Capture and Sequestration, Alexandria, VA, May 3-6.

García, J.E. (2003), *Fluid Dynamics of Carbon Dioxide Disposal Into Saline Aquifers,* PhD dissertation, U. of California at Berkeley, Berkeley, California, December.

IFC (International Formulation Committee) (1967), *A Formulation of the Thermodynamic Properties of Ordinary Water Substance,* IFC Secretariat, Düsseldorf, Germany.

Katz, D L. and R.L. Lee (1990), *Natural Gas Engineering,* McGraw-Hill, New York.

Kervevan Ch., M. Azaroual and P. Durst (2005). Improvement of the calculation accuracy of acid gas solubility in deep reservoir brines: application to the geological storage of CO_2. *Oil & Gas Sc. Techn.* Vol. 60, 357-379.

Pruess, K. (2004a), The TOUGH Codes—A Family of Simulation Tools for Multiphase Flow and Transport Processes in Permeable Media, *Vadose Zone J.,* Vol. 3, pp. 738 - 746.

Pruess, K. (2004b), Numerical Simulation of CO_2 Leakage from a Geologic Disposal Reservoir, Including Transitions from Super- to Sub-Critical Conditions, and Boiling of Liquid CO_2, *Soc. Pet. Eng. J.,* pp. 237 - 248, June.

Pruess, K. and J.E. García (2002), Multiphase Flow Dynamics during CO_2 Injection into Saline Aquifers, *Environmental Geology,* Vol. 42, pp. 282–295.

Pruess, K. and T.N. Narasimhan (1985), A Practical Method for Modeling Fluid and Heat Flow in Fractured Porous Media, *Soc. Pet. Eng. J.*, 25 (1), 14-26, February.

Ramey, H.J., Jr. (1962), Wellbore Heat Transmission, *J. Petrol. Tech.,* April 1962, pp. 427-435; *Trans., AIME,* Vol. 225.

Sanyal, S.K. and S.J. Butler (2005), An Analysis of Power Generation Prospects from Enhanced Geothermal Systems, *Proceedings, Paper 1632.pdf,* World Geothermal Congress 2005, Antalya, Turkey, 24-29 April.

Span, R. and W. Wagner (1996), A New Equation of State for Carbon Dioxide Covering the Fluid Region from the Triple-Point Temperature to 1100 K at Pressures up to 800 MPa, *J. Phys. Chem. Ref. Data,* Vol. 25, No. 6, pp. 1509 - 1596.

Vargaftik, N.B. (1975), *Tables on the Thermophysical Properties of Liquids and Gases*, 2nd Ed., John Wiley & Sons, New York, NY.

Vinsome, P.K.W. and J. Westerveld (1980), A Simple Method for Predicting Cap and Base Rock Heat Losses in Thermal Reservoir Simulators, *J. Canadian Pet. Tech.*, 19 (3), 87–90, July-September.

Xu, T., J.A. Apps and K. Pruess (2005), Mineral Sequestration of Carbon Dioxide in a Sandstone-Shale System, *Chemical Geology,* Vol. 217, pp. 295–318.